International Journal of Thermal Sciences 51 (2012) 7–15

Contents lists available at SciVerse ScienceDirect

International Journal of Thermal Sciences

journal homepage: www.elsevier.com/locate/ijts

Sequential inverse method implemented into CFD software for the estimation of a radiation boundary

Micael Boulet[a], Bernard Marcos[a,*], Christine Moresoli[b], Michel Dostie[c]

[a] Chemical Engineering and Biotechnological Engineering Department, University of Sherbrooke, Sherbrooke, QC J1K 2R1,Canada
[b] Chemical Engineering Department, University of Waterloo, Waterloo, ON N2L 3G1, Canada
[c] LTE Hydro-Quebec, Shawinigan, QC G9N 7N5, l, Canada

ARTICLE INFO

Article history:
Received 19 May 2011
Received in revised form
23 August 2011
Accepted 24 August 2011
Available online 22 September 2011

Keywords:
CFD
Inverse method
Oven
Sequential
Tikhonov regularization
Data filtering

ABSTRACT

An inverse method was implemented in commercial CFD software to estimate the wall temperature of a simplified baking oven from the initial estimate of an inert baking product temperature located in the oven. The transport phenomena were modeled with the energy equation, the RANS equation (Reynolds-Averaged Navier–Stokes), the *k*-epsilon realizable turbulence model and the S2S radiation model. The optimisation approach was used, by formulating an objective function. The proposed method was sequential and the objective function was minimized at every given time step. The minimization iterative process was introduced within the CFD solver loop, therefore solving both field variables and the inverse problem at once. To address the noisy input data, two techniques were compared: 1- Tikhonov regularization 2- pre-filtering of data and evaluated for two different bakery products. Results showed that the pre-filtering method provided more accurate estimates and avoided the need for a realistic initial estimate of the wall temperature.

1. Introduction

Computational Fluid Dynamics (CFD) techniques represent a promising approach for process intensification and energy efficiency of thermal processes such as industrial baking operations. The transport phenomena are decisive factors for baking processes; flow and temperature field are of prime interest and can be obtained from CFD modeling. Numerical predictions of flow and heat transfer in ovens by means of CFD opens up the possibility to optimize the design and operation, while excessive prototyping and experimentation can be avoided. Therdthai et al. [18] developed a three dimensional CFD transient model with a moving grid for an industrial baking process. Theirdthai model was able to simulate the effect of the oven load on the heat transfer in the oven chamber. Wong et al. [21] proposed a two dimensional CFD model for the study of the transient heat transfer in a baking oven chamber as well as the temperature distribution in the dough/bread. The most important boundary conditions were the high temperature walls of the oven that supply the heat to the process by means of radiation; Boulet et al. [5] proposed a three dimensional CFD model for pilot oven chamber and concluded that the boundary conditions of the system, the radiation wall surfaces, are difficult to estimate precisely and represent a limitation for efficient CFD modeling of ovens.

The validation of models relies on accurate experimental data. In the context of baking operations, experimental measurement systems are suitable for measurements within the system but not appropriate for measurements at the boundaries of the system. Furthermore, in industrial ovens, only a few thermocouples are present, making the estimation of the emitting wall temperature extremely difficult to obtain. As a consequence, industrial baking ovens can be viewed as a boundary inverse problem where the cause, the thermal boundary, is unknown while some effect, the temperature inside the domain, the oven, is available via measurements. Broadly speaking, the objective of inverse problems is the estimation of unknown parameters of a system from some measurements available in the system. This type of inverse problem is the opposite of the conventional CFD approach, the direct modeling, where full specification of the boundaries of the system are required for modeling.

Boundary Inverse heat transfer problems have been solved mainly from temperature measurements inside the system for a variety of applications other than baking operations. For example, Alestra et al. [1] analysed the heat fluxes on aerospace vehicles during their atmospheric re-entry from indirect temperature measurements. Cui et al. [8] presented an inverse radiation analysis to estimate the radiative property using the complex variable

* Corresponding author.
E-mail address: bernard.marcos@usherbrooke.ca (B. Marcos).

1290-0729/$ – see front matter © 2011 Elsevier Masson SAS. All rights reserved.
doi:10.1016/j.ijthermalsci.2011.08.015

Nomenclature

α	regularization parameter
f_c	cut-off frequency, hz
h	sensible enthalpy (kJ/kg)
k	iteration index
t	time, s
T_c	calculated temperature of inert baking product, K
T_i	exact temperature of inert baking product, K
T_m	measured temperature (synthetic) of the inert baking product, K
$T_{m,f}$	filtered measured temperature of the inert baking product, K
T_w	wall temperature (ceiling), K
$T_{w,i}$	exact wall temperature, K
T_w	wall temperature (ceiling), K
T_c	inert baking product temperature, K

differentiation method to compute the sensitivity equations. Le Bideau et al. [13] developed a simple instrument, a solid inert product containing a thermocouple and providing estimates of the heat flux in an infrared furnace that were analysed with an inverse method approach. An inverse method approach was considered for the investigation of the thermal resistance between the mould and the extruding ingot during the continuous casting of metals [15]. The most adequate location for the thermal sensors was identified by a sensitivity analysis and then used to calculate the thermal resistance. Sobotka et al. [17] determined thermal contact resistances by an inverse methodology. The inverse methodology required the computation of the adjoint system and possibly the sensitivity functions. The different systems (direct and adjoint) are solved with commercial multiphysics software COMSOL. The previous examples solved inverse heat conduction problem (IHCP) and the solution was obtained by manipulating the discretization of the governing equations.

The inverse heat conduction problem requires the knowledge of the velocity field and consequently solving of the continuity and Navier–Stokes equation. The inverse heat convection problem is more complex than IHCP. Zhang and Chen [22] presented an inverse CFD modeling approach for the identification of contaminant sources in closed systems. The velocity field was very simple and did require solving the Navier–Stokes equation. The diffusion transport equation was modified with the quasi-reversibility method and a special temporal discretization scheme was proposed for stability purposes. Their method was integrated in the commercial CFD software, FLUENT, as a user-defined function and the modified equation was solved backward in time to estimate the contaminant source location. Huang and Chen [12] solved a transient 3D inverse forced convection problem by incorporating a conjugate gradient method to the commercial CFD code CFX4.2 and taking advantages of the different geometries that were readily available in the commercial CFD code. In their method, the direct, adjoint and sensitivity functions were computed but assumed that the velocity field did not depend on the boundary heat flux. The boundary heat flux was estimated from the temperature measurements located downstream of the flow. Zhao et al. [23] proposed a conjugate gradient method to determine the boundary heat fluxes at the surface of an enclosed porous system. In their method, the direct, the adjoint and the sensitivity equations were solved with the SIMPLER algorithm and the pressure correction method. Their method also considered the momentum equations in the computation of the three systems (direct, adjoint and sensitivity). Zhao's method required the sequential computation of the direct system, the adjoint system and the sensitivity system. The computation of these three systems was included in an iterative optimisation loop related to the conjugate gradient method. Furthermore, the analytical computation of the adjoint system for the turbulent momentum equations was not an easy task. For the three previous studies, the inverse methods are embedded in the CFD code which is unusual for most IHCP.

The aim of this study was to solve an inverse heat conduction-radiation problem for a baking oven application and capitalize on the powerful modeling capacity of CFD software. The inverse problem was based on a single thermocouple measurement for the estimation of a single thermal emitting system boundary and conjugated with turbulent flow and convective heat transfer. The solution methodology resorted to a general purpose commercial CFD software combined with a unique and efficient custom-built function. The proposed approach did not require the computation of auxiliary system (adjoint or sensitivity) and did not require several solving of the direct system.

2. Problem description

The problem under study originates from industrial baking tunnel ovens where products circulate on a conveyor belt, uncooked at the inlet and exiting fully cooked. The energy input to the baking chamber is supplied by hot walls or by heating elements (such as natural gas burners). Radiation is typically the predominant mode of heat transfer [3,5,10]. The problem addressed in this study was the identification and development of a method for the estimation of the temperature and heat flux for these hot walls. The proposed method was to monitor the transient temperature of an inert baking product located in the oven as a substitution to an actual baking product. A similar experimental approach was used by Verboven et al. [19] and Mistry et al. [14] to validate the CFD modeling of static ovens. The objective of the method was to estimate the wall temperature from the temperature measurements of the inert baking product, a small solid object of aluminum with a thermocouple connected to a data logger of the temperature measurements as baking proceeded. The transient temperature of the inert baking product was the input data of the inverse problem method and the wall temperature was the output estimate.

3. Formulation of the problem

3.1. Geometry

The geometry of the chamber was 2D and regular for computational ease (Fig. 1). The length was smaller than actual industrial ovens (at least 20 m), but the height (distance between the floor and the ceiling) was similar to industrial conditions. The ceiling (upper wall) was the major source of radiation reaching the inert baking product. A stream of hot air entered from the left and exited on the right in the diagram. In contrast to industrial operations, the

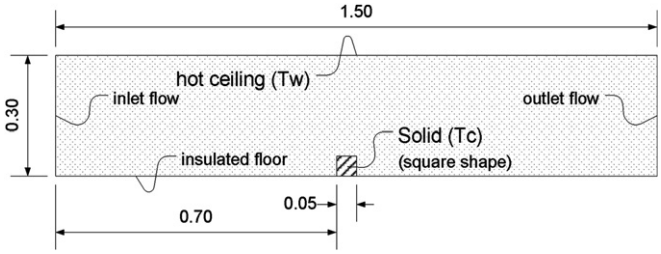

Fig. 1. Geometry of the inert baking product and baking oven considered in the model (dimension in meters).

inert baking product was introduced in the oven and remained stationary during the operation. A 2D computational methodology was selected for its ease and because of its good approximation of 3D industrial situations.

3.2. Transport phenomena mechanisms

The oven involved air flow and heat transfer mechanisms. The air flow was turbulent, as deduced by the estimation of the Reynolds number (Re). Given the operating velocity of 0.5 m/s, Re was about 7000. The three major heat transfer mechanisms, radiation, convection and conduction were considered. The air was assumed to be a non-participating media. That is, air did not absorb, emit or scatter radiation. Gravity effect was included; flow was in mixed-convection regime with the ratio of the Grashof and Reynolds numbers (Gr/Re) approximately unity.

4. Methodology

4.1. Direct problem modeling

4.1.1. Software and hardware

The Commercial software used for this study were FLUENT ver. 12.0 (solver) and Gambit ver. 2.4.6 (mesh generation), running on Microsoft Windows XP. The workstation was a Dell optiplex GX620, Pentium D 2.8 GHz, 4 GB ram.

4.1.2. Mathematical modeling

The turbulent air flow was modeled with the aim to predict the convective heat transfer on the inert baking product. The objective was not the details of the turbulent motion. Hence, RANS-based modeling approach was selected with the realizable $k-\varepsilon$ model as the air flow was impinging on the inert baking product. The realizable $k-\varepsilon$ model is a variant of the standard $k-\varepsilon$ model that is likely to perform better for situations with flow impinging on surfaces, since the turbulence energy may be over-predicted at the stagnation point [9].

The continuity and momentum equations written in the RANS format were (in summation convention):

$$\frac{\partial \rho}{\partial t}+\frac{\partial}{\partial x_i}(\rho u_i) = 0 \tag{1}$$

$$\frac{\partial}{\partial t}(\rho u_i)+\frac{\partial}{\partial x_j}(\rho u_i u_j) = -\frac{\partial p}{\partial x_i}+\frac{\partial}{\partial x_j}\left[\mu\left(\frac{\partial u_i}{\partial x_j}+\frac{\partial u_j}{\partial x_i}-\frac{2}{3}\delta_{ij}\frac{\partial u_l}{\partial x_l}\right)\right] + \rho\vec{g}+\frac{\partial}{\partial x_j}\left(-\rho\overline{u_i' u_j'}\right) \tag{2}$$

where density is a function of temperature following incompressible-ideal-gas law.

The *realizable* $k-\varepsilon$ model consists of the following two transport equations, one for the turbulence kinetic energy (k) and one for the dissipation rate (ε):

$$\frac{\partial}{\partial t}(\rho k)+\frac{\partial}{\partial x_j}(\rho k u_j) = \frac{\partial}{\partial x_j}\left[\left(\mu+\frac{\mu_t}{\sigma_k}\right)\frac{\partial k}{\partial x_j}\right]+G_k+G_b-\rho\varepsilon-Y_M \tag{3}$$

$$\frac{\partial}{\partial t}(\rho \varepsilon)+\frac{\partial}{\partial x_j}(\rho \varepsilon u_j) = \frac{\partial}{\partial x_j}\left[\left(\mu+\frac{\mu_t}{\sigma_\varepsilon}\right)\frac{\partial \varepsilon}{\partial x_j}\right]+\rho C_1 S_\varepsilon-\rho C_2\frac{\varepsilon^2}{k+\sqrt{\nu\varepsilon}} + C_{1\varepsilon}\frac{\varepsilon}{k}C_{3\varepsilon}G_b \tag{4}$$

Additional details of the realizable $k-\varepsilon$ model and the parameters can be found in ANSYS FLUENT Documentation [2] and Shih et al. [16].

The energy equation takes the form:

$$\frac{\partial}{\partial t}(\rho C_p T)+\frac{\partial}{\partial x_i}(u_i \rho h) = \frac{\partial}{\partial x_j}\left[\lambda\frac{\partial T}{\partial x_j}\right] \tag{5}$$

For the fluid region, the thermal conductivity, λ, becomes $(\lambda+\lambda_t)$ where λ_t is the turbulent thermal conductivity.

The radiation is the predominant heat transfer mechanism for industrial tunnel bakery ovens. For this study, the radiation was described with the *surface-to-surface* (S2S) model, a radiosity method that does not account for the contribution of the gaseous media:

$$J_i = E_i+(1-e_i)\sum_{j=1}^{N}F_{ij}J_j \tag{6}$$

where: J_i = radiosity (energy given off by surface i); E_i = emissive power of surface i; F_{ij} = fraction of energy leaving i and incident on j; e_i = emissivity of surface i.

For an N surface enclosure, the summation for each surface will generate N linear equations with N unknown radiosities.

4.1.3. Boundaries

Five different boundaries were defined, either wall or flow openings. The walls were:

- Inert baking product surface;
- ceiling;
- floor.

Flow openings were:

- inlet flow;
- outlet flow.

A summary of the boundary conditions is given in (Table 1).

The turbulence parameters at the inlet were approximated forms as follows [20]:

$$k = \frac{3}{2}\left(U_{ref}T_i\right)^2 \tag{7}$$

$$\varepsilon = C_\mu^{3/4}\frac{k^{3/2}}{l} \tag{8}$$

where: U_{ref} is the flow velocity; l is a length scale, taken as the height of the opening (0.3 m); T_{i} is the turbulence intensity, taken as 10%; $C_\mu = 0.09$.

The near-wall region was modeled with a low-Reynolds-number model and the two-layer approach proposed by Chen and Patel [7]. That opens up the possibility for the viscosity-affected near-wall region to be completely resolved up to the viscous sublayer, depending on the grid size. This approach was available in the software used, FLUENT 12.0, as the co-called "Enhanced Wall Treatment" option.

4.1.4. Numerical methods

The numerical procedure in FLUENT is based on the finite volume method. The solver has a segregated algorithm. That is, it solves for a single variable considering all cells at the same time using a point implicit (Gauss–Seidel) linear solver in combination with an AMG method. AMG is an Algebraic MultiGrid method that uses “virtual” coarse grid levels to accelerate convergence. The selected pressure-velocity coupling scheme was the SIMPLE algorithm. Spatial discretization formulations were as follows (face values interpolation):

- Gradient: Least square cells based
- Pressure: second order

Table 1
Boundary conditions of the oven and inert baking product illustrated in Fig. 1.

Equation	Inlet	Outlet	Ceiling	Inert baking product surface (exposed to fluid)	Floor
Energy	$T_{inlet}(t)$	(upwind scheme)	$T_w(t)$	coupled (conjugate heat transfer)	insulated
Radiation	$e = 0.90$	$e = 0.90$	$e = 0.90$	$e = 0.80$	$e = 0.90$
Momentum	velocity normal to boundary	$P = 1$ atm	no slip	no slip	no slip
Turbulence	$k = 0.0x$	(upwind scheme)	near-wall modeling	near-wall modeling	near-wall modeling
	$\varepsilon = 0.0x$				

- Momentum: second order upwind
- Turbulent kinematic energy: second order upwind
- Turbulent dissipation rate: second order upwind
- Energy: second order upwind

For the temporal discretization, the second order implicit formulation was selected.

4.1.5. Grid

Spatial discretization was achieved with an unstructured tetrahedral mesh. The cell size at the wall and in the near-wall region of the inert baking product was adjusted to allow resolution of the flow up to the viscous sublayer. This results in a dimensionless wall distance, $y+$, close to unity on those walls (boundaries of the inert baking product). Three different grid sizes were tested to confirm solution independence: 5785 cells; 7018 cells; 14 394 cells. All three grid sizes gave the same convective heat flux on object surface within 3% on average. However, flow pattern examination revealed that the coarse grid size had not the same characteristic recirculation zone (not the same size). Hence, the intermediate grid size (7018 cells) was chosen. Fig. 2 shows a view of the grid, including a close-up of the inert baking product.

4.1.6. Synthetic data generation

The data for the air temperature, the wall temperature and the inert product temperature for two different baking situations, a muffin and a tartlet, were obtained from the direct transient problem presented in our previous work [5] and are illustrated in Fig. 3. They reported that radiation was dominant and represented >75% of the total heat transfer.

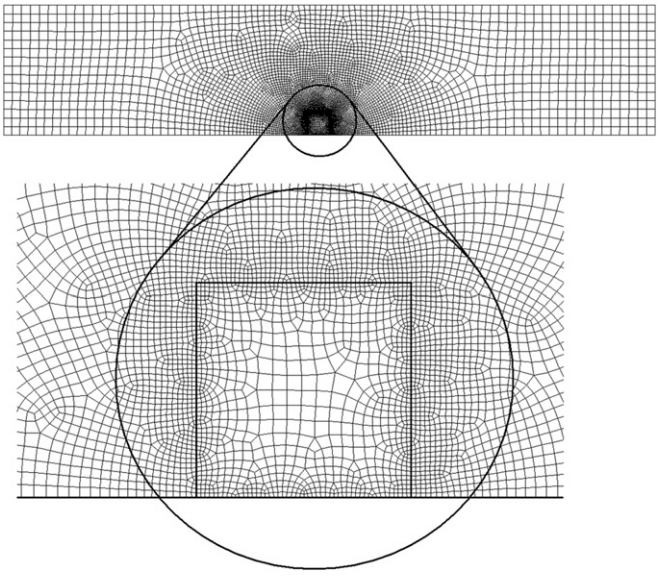

Fig. 2. Grid for spatial discretization.

A random noise was added to the exact temperature values of the inert baking product referred, the synthetic temperature data. A white noise with 0.5 Kelvin as maximum amplitude was chosen:

$$T_m = T_i + 2\cdot(\delta - \xi) \tag{9}$$

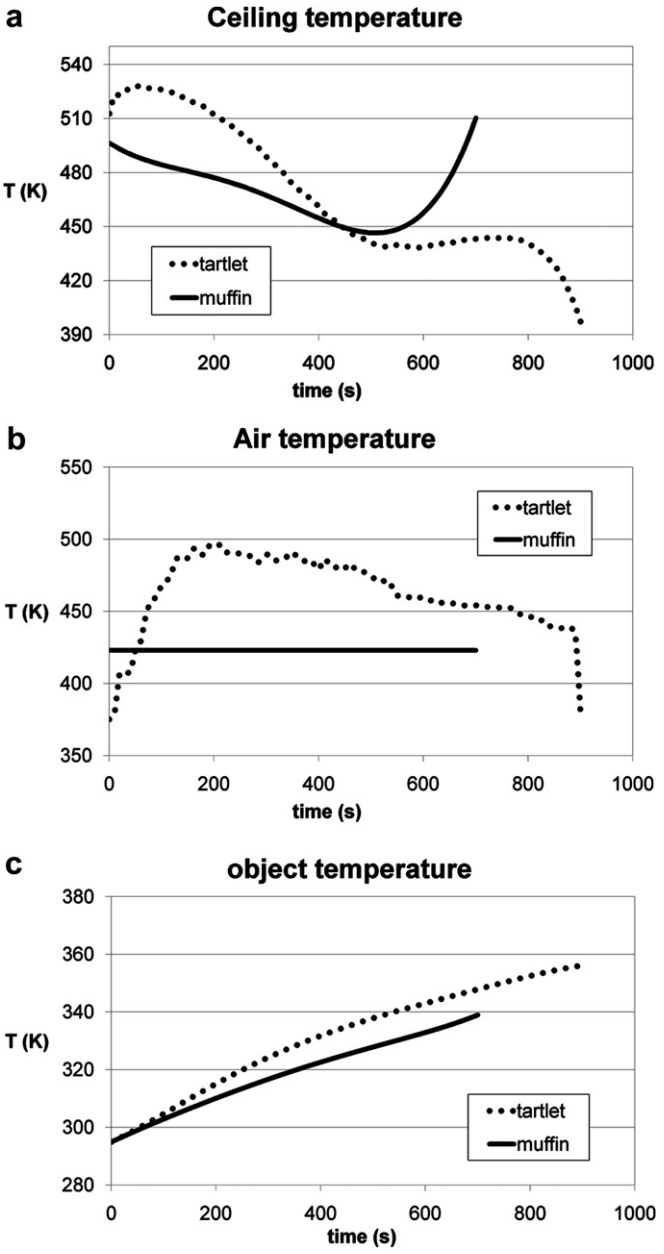

Fig. 3. Characteristics of the baking oven and two baking products investigated in this study. (A) Wall temperature of the oven; (B) Inlet air temperature; (C) Estimated temperature of the inert baking product from the direct simulation approach.

where T_m is the synthetic temperature data (synthetic measurement); T_i the exact product temperature value (direct problem solution, shown in Fig. 3C); ξ, the random number for the range [0,1]; δ, the maximum temperature measurement disturbance ($\delta = 0.5$).

4.2. Resolution by inverse method

The problem was inverted such that the known data became the experimental inert product temperature data (obtained by solving the direct problem) and the unknown data became the wall temperature, T_w (ceiling in Fig. 1). The predominant heat transfer that links these two temperatures is the thermal radiation. An important consideration with the radiation heat transfer mode is the heat leaving a wall will hit another wall in such a short time, not experimentally measurable i.e. considered instantaneous (practically speaking). The effect is sensitive (no lag), as opposed to the conductive heat transfer where the thermal response at some distance of the boundary is dampened and lagged. We took advantage of this characteristic by selecting a sequential method for solving the inverse problem. Sequential methods represent one of the two types of inverse methods for transient problems [6]. The second type of inverse methods, the global or "whole domain", methods would consider all the measured temperature data and estimate simultaneously all the components of the unknown input. In contrast, the sequential methods consider only a fraction of the available temperature data at a given step and only one component of the unknown input is estimated at a given step. In the sequential methods, an optimization problem will be solved at each time step. Starting with the initial conditions, the solution will be produced in a marching manner up to the final time. That is, only a fraction of the available temperature data will be used at each step and only one component of the unknown input will be estimated at each step. Such sequential methods have similarities with online control methods.

It is well known that inverse problems with noisy data are generally ill-posed and require specific methods to be solved. These specific methods provide regularized solutions leading to acceptable physical solutions. Recently, Bauer and Lukas [4] have compared several regularization approaches to solve linear inverse problems with noisy data. According to Bauer and Lukas [4], Tikhonov regularization and spectral cut-off (truncated singular value decomposition of the linear operator) regularization are the most popular regularization methods for such systems. The spectral cut-off method cannot be applied directly because of the non-linearity of the operator and the fundamental equations (momentum, energy). The Tikhonov regularization gives good results but the Tikhonov regularization performance may depend on the choice of the regularization parameter [4]. Furthermore, the filtering of data can also improve the efficiency of the regularization method.

4.2.1. Inert baking product data filtering – data preconditioning

Data smoothness can be improved by filtering. The technique proposed by Frankel and Arimilli [11], a low-pass Gauss filter, was selected in this work:

$$T_{m,f}(t) = \frac{\sum_{i=0}^{N} T_m \exp\left[-\left(\omega_c^2 (t-t_i)^2/4\right)\right]}{\sum_{i=0}^{N} \exp\left[-\left(\omega_c^2 (t-t_i)^2/4\right)\right]} \quad (10)$$

The parameter ω_c controls the width of the "bell" of the Gaussian function. The larger ω_c, the narrower the Gauss curve will be. The parameter ω_c is related to the cut-off frequency of the filter by the relation: $\omega_c = 2\pi f_c$. The appropriate value for ω_c is application specific.

For the problem under investigation, the inherent frequency (relevant content frequency) of the process was still visible in the noisy data. Indeed, there was an order of magnitude gap between the noise and the inherent signal in terms of frequency and magnitude. The frequency of the relevant content was estimated by visual inspection of the noisy data. Then a cut-off frequency was set corresponding to twice the inherent frequency.

As Frankel and Arimilli pointed out, pre- and post-padding of the data set are often considered to reduce leakage-type effects near the end points of the data set. The leakage at the end points was an important issue for the problem investigated in this study. Hence, pre- and post-padding consisting of the addition of 200 data points (200 s) at the beginning and at the end of the initial data set was included. The additional end points were obtained by extrapolation from the linear trend lines of the best fit for the first and last 30 s of the input data. A graphical example of this approach for the pre-padding is presented in Fig. 4. The approach was similar for the post-padding.

4.2.2. Tikhonov regularization method

As indicated earlier, the inverse problem was represented as an optimization problem by formulating an objective function. The noisy experimental data set of the inert baking product temperature gives a non-smooth function for the wall temperature. As inverse problems are ill-conditioned, the noise would further decrease the smoothness of the solution. An unsmooth solution is undesired from an operation perspective; the wall temperature cannot vary drastically for an actual oven. Hence, the objective function was formulated with the addition of a Tikhonov regularization component:

$$F(T_w(t_i)) = (T_m(t_i) - T_c(t_i))^2 + \alpha\left(\frac{T_w(t_i) - T_w(t_i - \Delta t)}{\Delta t}\right)^2 \quad (11)$$

The parameter α is the regularization parameter. The objective function contained two terms: the first term representing the fit between the measured temperature, T_m of the inert product, and the predicted temperature value, T_c of the inert product. The second term was the regularization term that restricts the variation of the wall temperature between the current time step and the previous time step. The regularization term contained a first order approximation dT_w/dt. This term is the so-called first order Tikhonov regularization, corresponding to the constraint that the solution is smooth (without sharp peaks).

The type of filter selected in this study gave smooth data after the application of the filter. Even though the filtered data did not fit exactly the initial data, there was no apparent noise remaining. Hence, no regularization was applied when the pre-filtered data were used and consequently, α was set equal to 0 in Eq. (11).

With the sequential approach, we seek to minimize F for each time t_i, where $i = 1, 2 \ldots N$ and N is the total number of time steps.

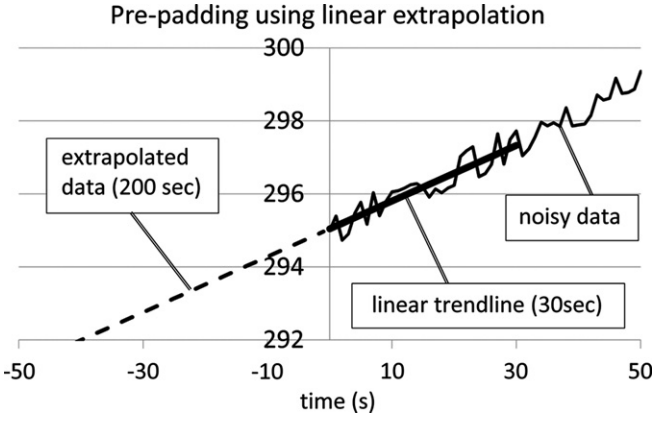

Fig. 4. Inverse problem iterative procedure at time t_i.

The Newton method was applied to minimize F. The implementation of the Newton method gave the following iterative process:

$$^{k+1}T_w(t_i) = {}^{k}T_w(t_i) - \left.\frac{F'}{F''}\right|_{t=t_i} \quad (12)$$

where superscript k denotes the iteration number. The first and the second derivatives of F with respect to T_w are given by:

$$F'|_{t=t_i} = -2[T_m(t_i) - T_c(t_i)] \left.\frac{\partial T_c}{\partial T_w}\right|_{t=t_i} + \frac{2\alpha}{\Delta t^2}(T_w(t_i) - T_w(t_i - \Delta t)) \quad (13)$$

$$F''|_{t=t_i} = -2[T_m(t_i) - T_c(t_i)] \left.\frac{\partial^2 T_c}{\partial {T_w}^2}\right|_{t=t_i} + 2\left(\left.\frac{\partial T_c}{\partial T_w}\right|_{t=t_i}\right)^2 + \frac{2\alpha}{\Delta t^2} \quad (14)$$

When α was set to zero, Eqs. (13) and (14) were simplified but the terms $\left.\frac{\partial T_c}{\partial T_w}\right|_{t=t_i}$ and $\left.\frac{\partial^2 T_c}{\partial T_w^2}\right|_{t=t_i}$ remained and represented the first order and second order sensitivities of the inverse problem (sensitivity of the output data with respect to the input data). The sensitivities should be estimated in order to perform the Newton–Raphson procedure.

Given the present phenomenological model (multiphysics), the derivation of sensitivity equation from the basic equations would involve excessive complexity. Instead, an approximate and very simple approach was selected to determine the sensitivities. The data set of T_c and T_w was fitted with a fourth order polynomial, such that the fourth power nature of the thermal radiation could be captured. The fit was very good and enabled the estimation of the first order and the second order sensitivities. This procedure was repeated for different times (step 1 above), and showed no significant dependence of the sensitivity with respect to T_c. Hence, the empirical formulation for the sensitivity was given as:

$$\left.\frac{\partial T_c}{\partial T_w}\right|_{t=t_i} = f(T_w) \quad (15)$$

$$f(T_w) = aT_w^3 + bT_w^2 + cT_w + d \quad (16)$$

With these estimations of the sensitivities, the Newton–Raphson procedure could be achieved. The values of T_c and T_w for a given time t_i were obtained by solving the direct problem from $(t_i - \Delta t)$ to time t_i. This was achieved by solving repeatedly the given time step Δt, but with a different T_w for each iteration and by taking the current system at iteration k as the initial conditions for the iteration $k+1$. The following lines sum up the Newton–Raphson procedure:

1) Solve the direct system to the time $(t_i - \Delta t)$.
2) Take the current system state as initial conditions $(t_i - \Delta t)$.
3) For the initial conditions, solve a single time step (ending at t_i) with a small wall temperature T_w. This step generates a set (T_c, T_w) at t_i.
4) Repeat step 3 to cover a wide and realistic range of T_w.
5) Compute the fourth order polynomial and the approximated sensitivities.
6) Compute the new wall temperature (Eq. (12)).
7) Compute the objective function F (Eq. (11)).
8) Return to 6), if the minimum is not reached.

4.2.3. Implementation into a CFD software

The iterative procedure given by the Newton method (Eq. (12)) was implemented in Fluent. Indeed, between two successive Newton iterations, the variable T_c was solved with the forward problem formulation and Fluent representing a closed loop calculation. With the sequential method, this procedure was applied for a single time step until convergence was reached. Then the time was incremented to the next time step and the procedure repeated again for this new time step.

The conventional CFD methodology used by Fluent is that the CFD solver iterates until convergence is obtained for a given $^{k}T_w$ before evaluating the next $^{k+1}T_w$ such that each time step is solved many times, hence being computationally demanding. Instead of this computationally demanding approach, we have developed a different and original approach which is much less computationally demanding. Indeed, we took advantage of the looping nature of the direct calculation procedure so that T_w could converge altogether with T_c (and all the field variables).

The conventional CFD procedure for solving the direct problem is depicted in Fig. 5A. By incorporating the proposed inverse method within the CFD solver iteration, it was possible to adjust T_w while the solver was actually solving the direct problem. That is, a single iteration of the CFD solver was followed by the evaluation of Eq. (12). In other words, the closed loop shown in Fig. 4 did not contain an inner loop in the CFD solver block. Hence, the convergence of T_w and all the other field variables were obtained simultaneously according to the procedure depicted in Fig. 5B.

The approach presented in Fig. 5B was implemented with subroutines (in C language). Each time a value of the wall temperature was required in the solver, a subroutine was called by the solver and a value of the wall temperature was calculated with Eq. (12).

The above procedure for solving the boundary inverse problem was tested with the data for two distinct baking product situations, a muffin and a tartlet and with

1) T_m as input data with a α = constant
2) $T_{m,f}$ as input data and $\alpha = 0$ (no regularization).

5. Results and discussion

5.1. Estimation of the regularization parameter

The regularization parameter α, Eq. (11), was determined with a parameter analysis, using one of the two baking product profiles. A number of simulations were performed with different α values. For each simulation, the error for the estimate of the wall temperature T_w was reported, in the least square sense. That is:

$$\text{error} = \sum_{i=1}^{N} (T_w(t_i) - T_{w,i}(t_i))^2 \quad (17)$$

Where $T_{w,i}(t)$ is the exact value of the wall temperature at time t_i estimated from the direct problem. Table 2 reports the error values for different α values as well as the average absolute deviation. The later was calculated with:

$$\text{average absolute deviation} = \frac{1}{N}\sum_{i=1}^{N} \left|T_w(t_i) - T_{w,i}(t_i)\right| \quad (18)$$

The optimal value for the regularization parameter value was found to be 0.028 for the muffin baking profile, as illustrated by the errors reported in Table 2. This value was then validated by applying the inverse method with regularization to the other product, the tartlet baking profile.

Fig. 6A and B present $T_w(t)$, the transient wall temperature profile estimated with the inverse method and $\alpha = 0.028$. For the

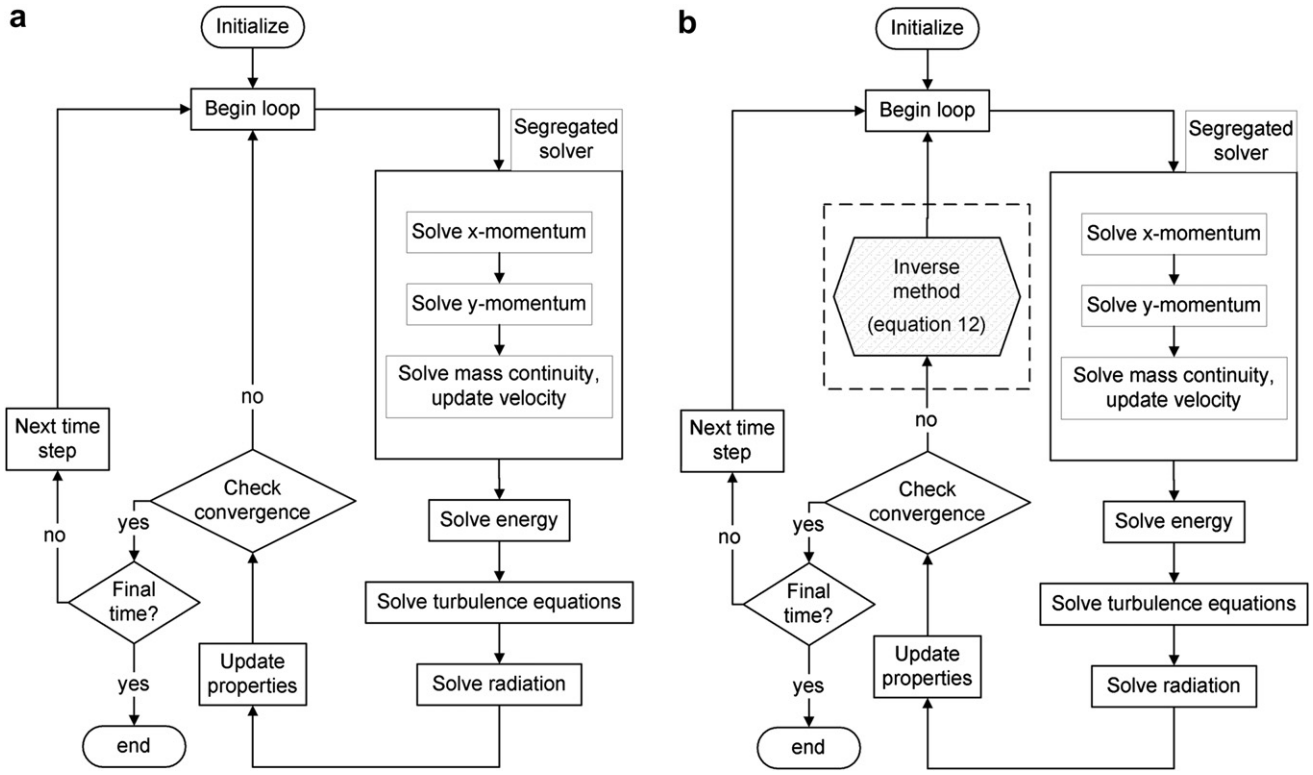

Fig. 5. Overview of (A) conventional CFD solution procedure and (B) Inverse method implemented into CFD procedure (---).

two products heating profiles investigated, the general behavior and the order of magnitude were correctly captured when compared to the exact values obtained for the direct problem. The estimated wall temperature profiles exhibited low frequency patterns, reminding of online control behaviour such as the PID controller.

An important consideration was the need for a realistic estimate of the initial condition, T_w $(t = 0)$. If the initial condition was inadequate, the model estimates were far from the value of the exact solution resulting in the amplification of the oscillation behaviour. Also, the frequency of the oscillations seemed to be related to the value of α. The lower the value of α, the higher was the frequency. Note that the results presented in Fig. 7 and Table 2 were obtained for the true values of the initial conditions.

5.2. Filtering approach

The inverse method was then assessed by considering filtered data ($T_{m,f}$) as input and posing $\alpha = 0$ with the same implementation approach. This method came from an attempt to eliminate the key

Table 2
Error estimates for the wall temperature for different regularization parameter values (proposed value highlighted).

Muffin case		
α	Error	Average absolute deviation (K)
0.01	59,200	23
0.02	7800	8.3
0.028	4500	6.8
0.03	4900	7.0
0.04	8400	7.6
0.05	1100	7.8

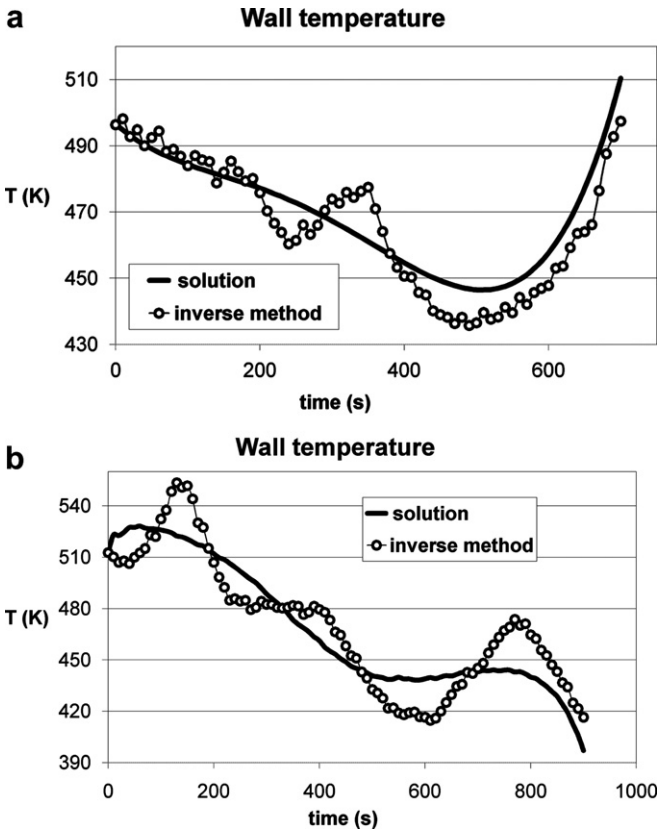

Fig. 6. Estimated wall temperature, T_w, profiles obtained with noisy input inert product temperature data, $\alpha = 0.028$. (A) Muffin; (B) Tartlet.

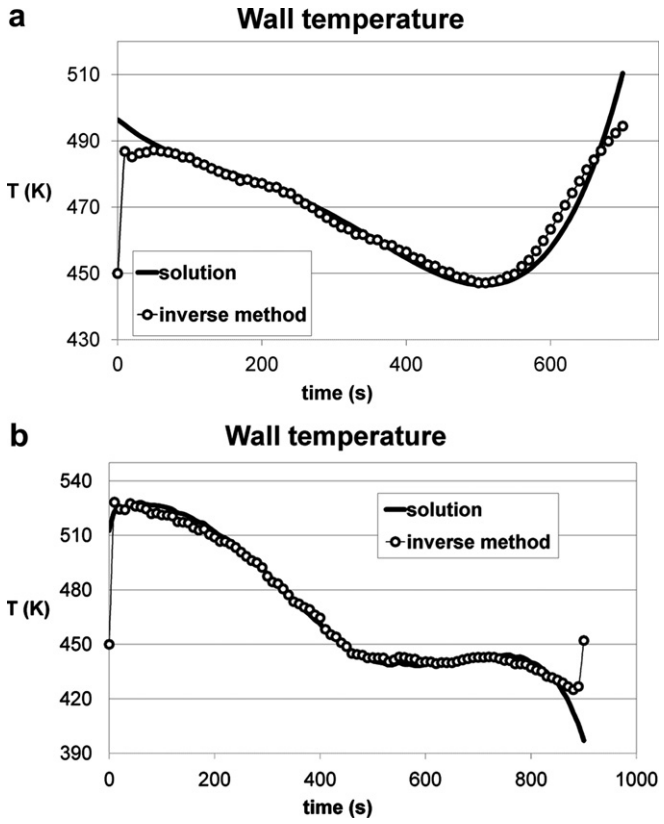

Fig. 7. Estimated wall temperature, T_w, profiles obtained with filtered input inert product temperature data. $\delta = 0.5$ filtered. (A) Muffin; (B) Tartlet.

drawback of the regularization method which requires a very good precise of the initial wall temperature condition. This is inherent to the first order Tikhonov regularization. However, by posing $\alpha = 0$, the requirement for a very smooth and wiggle-free input data was emphasized. This requirement could be avoided by considering the filtering of the input data. The estimates obtained with $\alpha = 0$ and pre-conditioned input data with the low-pass Gauss filter are reported on Fig. 7A and B. Even with a poor estimate of the initial wall temperature conditions (450 K), the estimates of the wall temperature profiles were very close to the true values obtained by the direct method and far better than the estimates obtained with the regularization method. Testing different initial estimates within realistic physical range (400–600 K) confirmed the independence of the solution with regard to the initial wall temperature.

The average deviation of the absolute product temperature was less than 3 K (2.8 K (muffin) and 2.9 K (tartlet)). The estimates near the initial and final baking times were less accurate. Though pre- and post-padding of the data set was used, results still exhibited the leakage behaviour inherent to the filter near the endpoints of the data set. This discrepancy confirmed the limitations of pre- and post-padding techniques to the data set prior to filtering.

Table 3
Relative number of iterations required for the estimation of the transient wall temperature.

Method	Relative number of iterations[a]	
	Muffin product	Tartlet product
direct problem	1.00	1.00
inverse problem with regularization	1.56	1.24
inverse problem with pre-filtered input data	1.83	1.33

[a] Relative to the number of iterations for solving the direct problem.

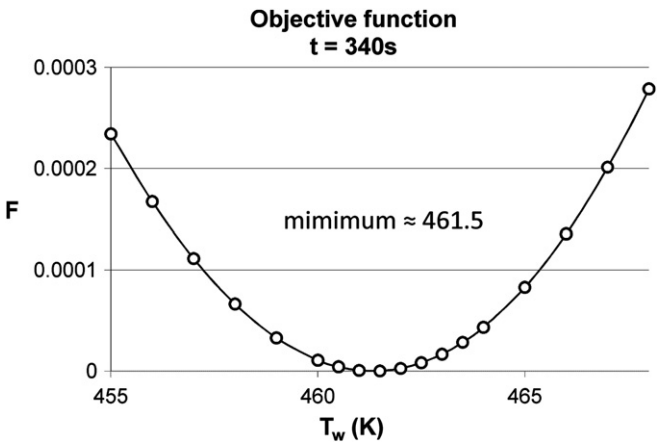

Fig. 8. Objective function numerically evaluated at 340 s for pre-filtered method and muffin product.

5.3. Convergence

From a CFD solver point of view, the wall thermal condition is a temperature input provided by the user. In our method, this "user" was the output from the algorithm that was different at each solver iteration. This approach introduced a numerical stress on the solver convergence. Still, as the variation of the wall condition became smaller at each new iteration, the convergence was expected to become stable. However, the inverse problem method required more iterations than for the direct problem method (Table 3). The inverse problem with the pre-filtered input data required more iterations than with the regularization for the muffin product.

The objective function (Eq. (11)) at a given time was analysed to assess the minimization process and to verify that the convergence of the algorithm was a minimum of the objective function. The time step from 330 s to 340 s was solved multiple times as a direct problem, changing T_w every time as employed previously for the sensitivity estimation. The initial wall temperature values at 330 s were taken from the simulation (at 330 s) obtained with the pre-filtered method and the heating profile of the muffin product. The objective function, $F(T_w)$ is shown in Fig. 8 for $\alpha = 0$. When selecting $\alpha = 0$, the minimum value for $F(T_w)$ was zero because the filtered measurement ($T_{m,f}$) could correspond to the calculated temperature (T_c). The minimum for these conditions was located around 462 K. This evaluation is consistent with the value obtained with the inverse problem simulation, as reported in Table 4.

Table 4
Report of T_w and dF/dT_w as iteration progressed at 340 s. Obtained with the inverse problem method and pre-filtered input data for the muffin product.

Iteration	T_w ($t = 340$ s)	dF/dT_w ($t = 340$ s)
Initial estimate	462.4	–
1	474.3	-1.47×10^{-4}
2	465.6	1.39×10^{-4}
3	459.9	8.17×10^{-5}
4	459.5	4.91×10^{-6}
5	461.0	-1.85×10^{-5}
6	461.7	-8.65×10^{-6}
7 (last)	461.6	8.97×10^{-7}

6. Conclusion

A commercial CFD software, primarily designed to solve direct problems, was successful in solving an inverse boundary problem for the estimation of a boundary radiating temperature profile (oven walls) by means of temperature data consisting of an inert baking object containing a temperature sensor and located in the oven. Taking advantage of the simplicity of the problem – a single sensor to estimate a single boundary condition – an original and efficient method was developed. Indeed, the time required for the resolution of the inverse problem was only 50% longer than the resolution of the direct problem. The proposed sequential inverse problem method involved the sequential minimization of an objective function one time step at a time. To address the noise in the input data, the first order Tikhonov regularization technique was selected and performed fairly well, though requiring a realistic estimate of the initial condition, the wall temperature. The pre-filtering of the input data provided more accurate estimates and avoided the need for a realistic initial estimate of the wall temperature. Future work should examine more sophisticated pre- and post-padding technique to improve the estimates near the endpoints of the input data set (early and late stage).

Acknowledgments

This project was carried out as part of the R&D program of the NSERC Chair in industrial energy efficiency (chair holder: Nicolas Galanis) established in 2006 at University of Sherbrooke with the support of Hydro-Quebec (Energy Technology Laboratory, LTE), Rio Tinto/Alcan International Ltd. and the CANMET Energy Technology Center (CETC-Varennes, Natural Ressources Canada).

References

[1] S. Alestra, J. Collinet, F. Dubois, An inverse method for non linear ablative thermics with experimentation of automatic differentiation, Journal of Physics: Conference Series 135 (2008) 012003.
[2] ANSYS FLUENT, 2009. 12.0-Theory Guide.
[3] O.D. Baik, M. Marcotte, F. Castaigne, Cake baking in tunnel type multi-zone industrial ovens part I. Characterization of baking conditions, Food Research International 33 (2000) 587–598.
[4] F. Bauer, M.A. Lukas, Comparing parameter choice methods for regularization of ill-posed problems, Mathematics and Computers in Simulation 81 (2010) 1795–1841.
[5] M. Boulet, B. Marcos, M. Dostie, C. Moresoli, CFD modeling of heat transfer and flow field in a bakery pilot oven, Journal of Food Engineering 97 (2010) 393–402.
[6] J.M.G. Cabeza, J.A.M. García, A.C. Rodríguez, A sequential algorithm of inverse heat conduction problems using singular value decomposition, International Journal of Thermal Sciences 44 (2005) 235–244.
[7] H.C. Chen, V.C. Patel, Near-wall turbulence models for complex flows including separation, AIAA Journal 26 (6) (1988) 641–648.
[8] M. Cui, X. Gao, H. Chen, Inverse radiation analysis in an absorbing, emitting and non-gray participating medium, International Journal of Thermal Sciences 50 (2011) 898–905.
[9] P.A. Durbin, On the k-3 stagnation point anomaly, International Journal of Heat and Fluid Flow 17 (1996) 89–90.
[10] D. Fahloul, G. Trystram, I. McFarlane, A. Duquenoy, Measurements and predictive modelling of heat fluxes in continuous baking ovens, Journal of Food Engineering 26 (1995) 469–479.
[11] J.I. Frankel, R.V. Arimilli, Inferring convective and radiative heating loads from transient surface temperature measurements in the half-space, Inverse Problems in Science and Engineering 15 (2007) 463–488.
[12] C.-H. Huang, W.-C. Chen, A three-dimensional inverse forced convection problem in estimating surface heat flux by conjugate gradient method, International Journal of Heat and Mass Transfer 43 (2000) 3171–3181.
[13] P. Le Bideau, J.P. Ploteau, P. Glouannec, Heat flux estimation in an infrared experimental furnace using an inverse method, Applied Thermal Engineering 29 (2009) 2977–2982.
[14] H. Mistry, Ganapathi-subbu, S. Dey, P. Bishnoi, J.L. Castillo, Modeling of transient natural convection heat transfer in electrical ovens, Applied Thermal Engineering 26 (2006) 2448–2456.
[15] A. Nawrat, J. Skorek, Inverse approach and sensitivity analysis for identification of ingot-mould thermal resistance in continuous casting of metals, International Journal of Computational Fluid Dynamics 19 (2005) 429–436.
[16] T.-H. Shih, W.W. Liou, A. Shabbir, Z. Yang, J. Zhu, A new k-ε eddy-viscosity model for high reynolds number turbulent flows – model development and validation, Computers and Fluids 24 (3) (1995) 227–238.
[17] V. Sobotka, N. Lefevre, Y. Jarny, D. Delaunay, Inverse methodology to determine mold set-point temperature in resin transfer molding process, International Journal of Thermal Sciences 49 (2010) 2138–2147.
[18] N. Therdthai, W. Zhou, T. Adamczak, Three-dimensional CFD modelling and simulation of the temperature profiles and airflow patterns during a continuous industrial baking process, Journal of Food Engineering 65 (2004) 599–608.
[19] P. Verboven, N. Scheerlinck, J. De Baerdemaeker, B.M. Nicolai, Computational fluid dynamics modeling and validation of the temperature distribution in a forced convection oven, Journal of Food Engineering 43 (2000) 61–73.
[20] H.K. Versteeg, W. Malalasekera, An Introduction to Computational Fluid Dynamics, the Finite Volume Method. Longman Scientific and Technical, England, 1995.
[21] S.Y. Wong, W. Zhou, J. Hua, CFD modeling of an industrial continuous bread-baking process involving U-movement, Journal of Food Engineering 78 (2007) 888–896.
[22] T.F. Zhang, Q. Chen, Identification of contaminant sources in enclosed environments by inverse CFD modeling, Indoor Air 17 (2007) 167–177.
[23] F.-Y. Zhao, D. Liu, G.-F. Tang, Numerical determination of boundary heat fluxes in an enclosure dynamically with natural convection through Fletcher–Reeves gradient method, Computers and Fluids 38 (2009) 797–809.